

Robust Forecasting-Aided State Estimation for Power System Against Uncertainties

Yi Wang , Student Member, IEEE, Yonghui Sun , Member, IEEE, and Venkata Dinavahi , Senior Member, IEEE

Abstract—Accurate forecasting-aided state estimation plays a vital role in reliable and secure operation of power systems. However, most of existing methods are unable to deal with the uncertainties that might be caused by uncertain model parameters or uncertain noise statistics. Therefore, the performance of these methods may be inevitably degraded significantly. To address these issues, based on the robust control theory, in this paper, by incorporating the modified innovation based Sage-Husa estimator of noise statistics and the proposed estimation error covariance matrix adaptive technique, a novel adaptive H_∞ extended Kalman filter (AHEKF) is developed to realize robust forecasting-aided state estimation for power system with model uncertainties. Extensive simulations carried out on several different test systems demonstrate the efficiency and robustness of the proposed method.

Index Terms—Model uncertainties, extended Kalman filter, H_∞ filter theory, forecasting-aided state estimation.

LIST OF ACRONYMS

SE	State estimation.
DSE	Dynamic state estimation.
EKF	Extended Kalman filter.
IEKF	Iterated extended Kalman filter.
UKF	Unscented Kalman filter.
PF	Particle filter.
HEKF	H_∞ extended Kalman filter.
AHEKF	Adaptive H_∞ extended Kalman filter.

I. INTRODUCTION

ACCURATE state estimation of power system plays an important role in secure and reliable operation of power

Manuscript received February 4, 2019; revised April 9, 2019 and July 11, 2019; accepted August 13, 2019. Date of publication August 19, 2019; date of current version January 7, 2020. This work was supported in part by the National Natural Science Foundation of China under Grant 61673161, in part by the Natural Science Foundation of Jiangsu Province of China under Grant BK20161510, in part by the Six Talent Peaks High Level Project of Jiangsu Province under Grant 2017-XNY-004, and in part by the Natural Science and Engineering Research Council (NSERC) of Canada. The work of Y. Wang was supported by the China Scholarship Council. Paper no. TPWRS-00184-2019. (Corresponding author: Yonghui Sun.)

Y. Wang is with the College of Energy and Electrical Engineering, Hohai University, Nanjing 210098, China, and also with the Department of Electrical and Computer Engineering, University of Alberta, Edmonton, AB T6G 2V4, Canada (e-mail: wangyi1414599008@163.com).

Y. Sun is with the College of Energy and Electrical Engineering, Hohai University, Nanjing 210098, China (e-mail: sunyonghui168@gmail.com).

V. Dinavahi is with the Department of Electrical and Computer Engineering, University of Alberta, Edmonton, AB T6G 2V4, Canada (e-mail: dinavahi@ualberta.ca).

Digital Object Identifier 10.1109/TPWRS.2019.2936141

systems, since it can provide the vital information for system monitoring and control [1]. The states of power system are generally estimated by the traditional static SE approach utilizing redundant measurements [2]. Static SE method exhibits the characteristics of simplified implementation and fast convergence, but it regards the current state as only related to present measurements and ignores the dynamics of power system. In fact, due to the continuous variations in loads and generators, the state of the system changes slowly with time rather than being static [3]. In addition, with increasing number of wind farms integrated into power grid, the stochastic and intermittent characteristics inevitably increase the probability of bus voltage phasor suddenly changing during a short time. As a result, the estimation results obtained by utilizing static SE methods may not effectively and accurately reflect the actual operation states of power system.

In recent years, to overcome the drawbacks of static SE, significant attention has been paid to the design of forecasting-aided SE (some researchers also call it DSE [4]) for power systems. Up to date, a variety of useful approaches have been developed, which are mainly based on Kalman filter [5]–[13]. In [5], by using the terminal reactive power, active power, frequency, and voltage phasor measurements from PMUs, a decentralized extended Kalman filter with unknown inputs method was developed to accurately estimate the states of the synchronous machine in multi-machine power systems. In [6], based on the generalized maximum likelihood method, by incorporating the traditional EKF, a robust IEKF approach was proposed. The method exhibits robustness to innovation and observation outliers. In [7], a new method was developed to calculate the state transition matrix of power system, which enhanced the accuracy of DSE. In [8], based on the EKF algorithm, a placement strategy was proposed for the number and locations of PMUs installed in the system to guarantee satisfactory state estimation results. Further, in order to circumvent the approximation errors introduced by linearization in conventional EKF, other nonlinear filters have also been developed and utilized in power system dynamic state estimation, such as the UKF [9]–[12] and the PF [13].

Based on the above analysis, it can be seen that Kalman-type filters play an important role in power system dynamic state estimation. However, it should be noted that most of the aforementioned methods assume that the complete knowledge of DSE model is available, which means that these approaches work well only while certain conditions are satisfied [14]–[20]. First, the state-space model is assumed to be known accurately, such as all

the model parameters can be acquired exactly. Second, the noise statistics of process noise and measurement noise are assumed to be known in advance, wherein their covariance matrices can be calculated exactly; the reason is that the performance of Kalman-type filters are highly affected by the covariance matrices of noise [21]–[24]. However, for a practical power system, these assumptions might not be valid in most cases. One reason is that the noise statistics of process noise and measurement noise may be difficult to be obtained, due to both of them being heavily affected by the real operating conditions of power system that change dynamically; the other reason is that some nonlinearities may not be modeled. These model uncertainties inevitably degrade the estimation performance of aforementioned Kalman-type filters, and significantly biased estimation results might be obtained.

In order to mitigate the adverse effects of model uncertainties, some robust dynamic state estimation approaches for power system were proposed in [20], [23]. Specifically, by using the generalized likelihood estimator, a robust unscented Kalman filter method for power system DSE was proposed in [20], which exhibited a robustness to unknown noise statistics. Recently, based on H_∞ filter, a new approach for power system DSE considering the model uncertainties was developed in [19], which could realize the DSE of power system under the given finite upper bound of the model uncertainties. However, it should be pointed out that, the covariance matrices of system noise and measurement noise are still assumed to be constants during the process of dynamic state estimation, thus their dynamic feature of changing with time is not taken into account. In addition, in this method, the finite upper bound of the model uncertainties need to be set up artificially, which might be difficult to choose the appropriate value of it for real applications. Thus, the practical value of the proposed method would be hampered.

To address these issues, in this paper, a novel adaptive H_∞ extended Kalman filter is developed to realize robust forecasting-aided state estimation for power system with model uncertainties. At first, an adaptive strategy is proposed to automatically tune the estimation error covariance matrix corresponding to the changeable conditions. Then the difficulty of choosing an suitable upper bound of estimation error is avoided, and a better robust behavior can be obtained. In addition, a modified innovation based Sage-Husa estimator of noise statistics is also adopted to dynamically calculate the covariance matrices of system noise and measurement noise. Finally, extensive test results of IEEE 14, 30, 57, and 118-bus are provided to demonstrate the effectiveness and robustness of the proposed method.

The remainder of this paper is organized as follows. In Section II, the state-space model of power system is presented. In Section III, the proposed adaptive H_∞ extended Kalman filter approach is introduced in detail. In Section IV, results of the extensive simulations carried out on several test systems are provided to demonstrate the efficacy of the proposed method, and finally the conclusions are drawn in Section V.

Notation: The notation utilized here is fairly standard except where otherwise stated. $\tilde{\mathbf{x}}_k$ and $\hat{\mathbf{x}}_k$ indicate the predicted and estimated state vector at time instant k , respectively. \mathbf{z}_k represents the measurement at time instant k . \mathbf{F}_{k-1} denotes

the state transition matrix at time instant $k - 1$. \mathbf{I} denotes the identity matrix with appropriate dimension. $E[\mathbf{x}]$ stands for the expectation of the stochastic variable \mathbf{x} . \mathbf{K}_k represents the Kalman gain at time instant k . $\hat{\boldsymbol{\xi}}_k$ and $\hat{\mathbf{R}}_k$ are the estimated covariance matrices of process noise and measurement noise at time instant k , respectively.

II. STATE-SPACE MODEL OF POWER SYSTEM

In this section, the general discrete time state-space model of power system is described. Then, the state transition model represented by Holt's exponential smoothing technique is discussed. Finally, the different types of measurements are analyzed, and the specific nonlinear measurement model is presented.

A. Discrete Time State-Space Model

In general, the discrete time state and measurement equations of a dynamical power system can be described by

$$\mathbf{x}_k = \mathbf{f}(\mathbf{x}_{k-1}) + \mathbf{w}_k, \quad (1)$$

$$\mathbf{z}_k = \mathbf{h}(\mathbf{x}_k) + \mathbf{v}_k, \quad (2)$$

where the subscripts k and $k - 1$ are two successive discrete time instants separated by a sample period T . $\mathbf{f}(\cdot)$ and $\mathbf{h}(\cdot)$ are the system function and the measurement function, respectively, both of them can be linearized by Taylor series expansion. \mathbf{x}_k denotes the state vector, \mathbf{z}_k is the measurement vector, \mathbf{w}_k represents the Gaussian system noise with zero mean and the covariance $\boldsymbol{\xi}_k$, \mathbf{v}_k indicates the Gaussian measurement noise with zero mean and the covariance \mathbf{R}_k .

B. State Transition Model

In this brief, the power system is assumed to operate under the quasi-steady state, where loads and generators do not have large sudden changes [27]–[29]. Note that such kind of steady-state dynamics is typically different from the transient ones might be caused by the large disturbances, such as cyber-attack, short circuit faults, to cite a few [1]. In order to reflect the dynamic changes of power system, several state transition models have been investigated in [25]–[28]. Among them, the one that expressed by the Holt's exponential smoothing technique is the most widely utilized [37].

By utilizing the Holt's exponential smoothing technique, the state transition function $\mathbf{f}(\cdot)$ in (1) can be expressed by

$$\mathbf{f}(\mathbf{x}_{k-1}) = \mathbf{a}_{k-1} + \mathbf{b}_{k-1}, \quad (3)$$

where \mathbf{a}_{k-1} and \mathbf{b}_{k-1} are respectively the horizontal component and the inclined component at time instant $k - 1$, which are recursively defined as follows

$$\mathbf{a}_{k-1} = \alpha \mathbf{x}_{k-1} + (1 - \alpha) \tilde{\mathbf{x}}_{k-1}, \quad (4)$$

$$\mathbf{b}_{k-1} = \beta (\mathbf{a}_{k-1} - \mathbf{a}_{k-2}) + (1 - \beta) \mathbf{b}_{k-2}, \quad (5)$$

where α and β are the two different smoothing parameters with values between 0 and 1. \mathbf{x}_{k-1} and $\tilde{\mathbf{x}}_{k-1}$ represent the true state vector, the predicted state vector at time instant $k - 1$, respectively.

Then, by substituting (4), (5) into (3) and considering the system noise, the general form of state transition model can be derived as follows [25]

$$\mathbf{x}_k = \mathbf{F}_{k-1}\mathbf{x}_{k-1} + \mathbf{G}_{k-1} + \mathbf{w}_{k-1}, \quad (6)$$

where

$$\mathbf{F}_{k-1} = \alpha(1 + \beta)\mathbf{I}, \quad (7)$$

$$\mathbf{G}_{k-1} = (1 + \beta)(1 - \alpha)\tilde{\mathbf{x}}_{k-1} - \beta\mathbf{a}_{k-2} + (1 - \beta)\mathbf{b}_{k-2}, \quad (8)$$

where \mathbf{F}_{k-1} denotes the state transition matrix, \mathbf{G}_{k-1} indicates the parameter vector; \mathbf{I} represents the identity matrix with corresponding dimension. More detailed information about this model can be found in [25].

In addition, it is worth pointing out that the state vector to be estimated in forecasting-aided state estimation consists of voltage phase angle and amplitude at each node, which is defined as follows

$$\mathbf{x}_k = [\theta_{2,k}, \theta_{3,k}, \dots, \theta_{N,k}, V_{1,k}, V_{2,k}, \dots, V_{N,k}]^T, \quad (9)$$

where the subscript N denotes the total number of nodes in a power system, $\theta_{i,k}$ (in radians) represents the phase angle at bus i and time instant k , $V_{i,k}$ indicates the voltage magnitude at bus i and time instant k . Note that $\theta_{1,k}$ acts as the reference phase, which is not considered in the state vector to be estimated.

C. Measurement Model

For forecasting-aided state estimation of power system, the following noise-contaminated measurements are utilized, which consists of the voltage magnitude, active and reactive power injections at buses, denoted as $\mathbf{V}_k = [V_{1,k}, \dots, V_{n_v,k}]$, $\mathbf{P}_k = [P_{1,k}, \dots, P_{n_p,k}]$, and $\mathbf{Q}_k = [Q_{1,k}, \dots, Q_{n_p,k}]$, respectively; and the active power flow measurements $\mathbf{P}_k^f = [P_{1,k}^f, \dots, P_{n_l,k}^f]$, the reactive power flow measurements $\mathbf{Q}_k^f = [Q_{1,k}^f, \dots, Q_{n_l,k}^f]$ [29]. Suppose all the measurements are collected, then the nonlinear measurement model in (2) can be expressed as

$$\mathbf{z}_k = [\mathbf{V}_k \ \mathbf{P}_k \ \mathbf{Q}_k \ \mathbf{P}_k^f \ \mathbf{Q}_k^f]^T + \mathbf{v}_k. \quad (10)$$

By utilizing the general two-port π -model of network branches [30], the precise elements for the measurements \mathbf{P}_k , \mathbf{Q}_k , \mathbf{P}_k^f , \mathbf{Q}_k^f are given as follows (for brevity, the time subscript k is omitted):

$$P_i = \sum_{j=1}^N |V_i||V_j|(G_{ij} \cos \theta_{ij} + B_{ij} \sin \theta_{ij}), \quad (11)$$

$$Q_i = \sum_{j=1}^N |V_i||V_j|(G_{ij} \sin \theta_{ij} - B_{ij} \cos \theta_{ij}), \quad (12)$$

$$P_{ij} = V_i^2(G_{si} + G_{ij}) - |V_i||V_j|(G_{ij} \cos \theta_{ij} + B_{ij} \sin \theta_{ij}), \quad (13)$$

$$Q_{ij} = -V_i^2(B_{si} + B_{ij}) - |V_i||V_j|(G_{ij} \sin \theta_{ij} - B_{ij} \cos \theta_{ij}), \quad (14)$$

where P_i and Q_i denote the active power and reactive power injections at bus i ; P_{ij} and Q_{ij} represent the real power flow, the reactive power flow between buses i and j , respectively; V_i indicates the voltage magnitude of bus i ; G_{ij} , B_{ij} denote the conductance and the susceptance of the line between i and j , respectively; G_{si} and B_{si} indicate the conductance, the susceptance of the shunt at bus i , respectively.

Remark 1: The power system model expressed by (6) and (10) has been widely utilized in many forecasting-aided state estimation studies [25]–[27], in most of these research, both the model parameters and the noise statistics are usually assumed to be known accurately in advance. However, for a practical power system, some model parameters are difficult to obtain exactly (such as the smoothing parameters α , β) and the noise statistics maybe unknown. These uncertainties inevitably affect the performance of the conventional state estimator, yielding significantly biased estimation results [2], [19]. To deal with these problems, a robust forecasting-aided state estimation method for power system against uncertainties will be designed in the next section.

III. PROPOSED ADAPTIVE H_∞ EXTENDED KALMAN FILTER

In this section, the criteria for bounding the state estimation error caused by model uncertainties is introduced. Then, by using the criteria, the main steps to develop the adaptive H_∞ extended Kalman filter are presented in detail.

A. Criteria for Model Uncertainties

The model uncertainties inevitably degrade the performance of conventional forecasting-aided state estimation methods significantly. In order to deal with this problem, based on the robust control theory [17], a criteria that derives the finite upper bound on the state estimation error can be established as follows [19], [31]

$$\lambda^2 \geq \sup_{\{\mathbf{x}_0, \mathbf{v}_k, \mathbf{w}_k\}} \frac{\sum_{k=0}^{N_t-1} \|\mathbf{x}_k - \hat{\mathbf{x}}_k\|_{\hat{\mathbf{P}}_k}^2}{\|\mathbf{x}_0 - \hat{\mathbf{x}}_0\|_{\hat{\mathbf{P}}_0}^2 + \sum_{k=0}^{N_t-1} \left(\|\mathbf{w}_k\|_{\hat{\boldsymbol{\xi}}_k}^2 + \|\mathbf{v}_k\|_{\hat{\mathbf{R}}_k}^2 \right)}, \quad (15)$$

where $\lambda > 0$ represents the attenuation level that bounds on the estimation error, N_t denotes the number of measurements, \mathbf{x}_k is the true state vector, $\hat{\mathbf{x}}_k$ indicates the estimation result of \mathbf{x}_k ; $\hat{\mathbf{P}}_0$ is the initial state estimation covariance matrix, $\hat{\mathbf{P}}_k$ represents the state estimation covariance matrix at time instant k . $\hat{\boldsymbol{\xi}}_k$ and $\hat{\mathbf{R}}_k$ are the respective covariance matrices of process noise and measurement noise at time instant k , which could be estimated by the method introduced in Part C of this Section.

B. Adaptive H_∞ Extended Kalman filter

In order to obtain a more accurate and reliable dynamic state estimation result of power system, which could suppress the adverse effects of model uncertainties on the accuracy of estimation result, in this part, a robust forecasting-aided state

estimation approach, named as adaptive H_∞ extended Kalman filter is designed.

By utilizing the criteria (15), the adaptive H_∞ extended Kalman filter for robust forecasting-aided power system state estimation against model uncertainties can be implemented by the following consecutive steps:

1) Parameter Identification

In order to utilize the linear state transition model in (6), at first, the parameter matrices of \mathbf{F}_{k-1} and \mathbf{G}_{k-1} need to be identified by utilizing the linear exponential smoothing technique that expressed in (4), (5), (7) and (8).

2) Initialization

In this stage, in order to predict the states of the power system, the values of state vector $\hat{\mathbf{x}}_0$ and the state estimation error covariance matrix $\hat{\mathbf{P}}_0$ should be initialized in advance, which can be computed as

$$\hat{\mathbf{x}}_0 = E[\mathbf{x}_0], \quad (16)$$

$$\hat{\mathbf{P}}_0 = E[(\mathbf{x}_0 - \hat{\mathbf{x}}_0)(\mathbf{x}_0 - \hat{\mathbf{x}}_0)^T]. \quad (17)$$

3) State Prediction

The prediction state vector $\tilde{\mathbf{x}}_k$ and corresponding prediction error covariance matrix $\tilde{\mathbf{P}}_k$ at time instant k can be formulated as

$$\tilde{\mathbf{x}}_k = \mathbf{F}_{k-1}\hat{\mathbf{x}}_{k-1} + \mathbf{G}_{k-1}, \quad (18)$$

$$\tilde{\mathbf{P}}_k = \mathbf{F}_{k-1}\hat{\mathbf{P}}_{k-1}\mathbf{F}_{k-1}^T + \hat{\boldsymbol{\xi}}_{k-1}, \quad (19)$$

where $\hat{\mathbf{P}}_{k-1}$ and $\hat{\mathbf{x}}_{k-1}$ represent the state estimation error covariance matrix and the estimated state at time instant $k-1$, respectively.

4) State Update

In this step, the predicted state vector $\tilde{\mathbf{x}}_k$ can be updated by using the new set of measurement \mathbf{z}_k , which can be calculated by

$$\hat{\mathbf{x}}_k = \tilde{\mathbf{x}}_k + \mathbf{K}_k[\mathbf{z}_k - \mathbf{h}(\tilde{\mathbf{x}}_k)], \quad (20)$$

where Kalman filter gain \mathbf{K}_k is expressed as

$$\mathbf{H}_k = \left. \frac{\partial \mathbf{h}(\mathbf{x}_k)}{\partial \mathbf{x}_k} \right|_{\mathbf{x}_k = \tilde{\mathbf{x}}_k}, \quad (21)$$

$$\mathbf{K}_k = \tilde{\mathbf{P}}_k \mathbf{H}_k^T (\mathbf{H}_k \tilde{\mathbf{P}}_k \mathbf{H}_k^T + \hat{\mathbf{R}}_k)^{-1}, \quad (22)$$

where \mathbf{H}_k denotes the Jacobian matrix of the measurement function $\mathbf{h}(\cdot)$ at time instant k .

5) Adaptive Update of Estimation Error Covariance Matrix

Now, in order to guarantee the boundedness of the estimation error, following the criteria (15), the estimation error covariance matrix $\hat{\mathbf{P}}_k$ is designed as follows (detailed derivation process of it can be seen in the part A of Appendix)

$$\hat{\mathbf{P}}_k = \begin{cases} (\mathbf{I} - \mathbf{K}_k \mathbf{H}_k) \tilde{\mathbf{P}}_k & \text{if } P_{z,k} > \alpha \bar{P}_{z,k}, \\ (\boldsymbol{\eta}_k - \lambda^{-2} \mathbf{L}_k^T \mathbf{L}_k)^{-1} & \text{otherwise,} \end{cases} \quad (23)$$

where $\bar{P}_{z,k} = E(\bar{\mathbf{z}}_k \bar{\mathbf{z}}_k^T | \tilde{\mathbf{x}}_{k-1})$ denotes the real covariance matrix of the innovation $\bar{\mathbf{z}}_k = \mathbf{z}_k - \mathbf{h}(\tilde{\mathbf{x}}_k)$ at time instant k , $\alpha > 0$ is a scalar parameter that provides an extra degree of the freedom to tune the threshold in the process of implementation, $\boldsymbol{\eta}_k$ and

$\mathbf{P}_{z,k}$ are calculated by

$$\boldsymbol{\eta}_k = \tilde{\mathbf{P}}_k^{-1} + \mathbf{H}_k^T \hat{\mathbf{R}}_k^{-1} \mathbf{H}_k, \quad (24)$$

$$\mathbf{P}_{z,k} = \mathbf{H}_k \tilde{\mathbf{P}}_k \mathbf{H}_k^T + \hat{\mathbf{R}}_k. \quad (25)$$

In addition, $\bar{P}_{z,k}$ can be estimated by [31]

$$\bar{P}_{z,k} = \begin{cases} \bar{\mathbf{z}}_k \bar{\mathbf{z}}_k^T, & \text{if } k = 0, \\ \frac{\rho \bar{P}_{z,k-1} + \bar{\mathbf{z}}_k \bar{\mathbf{z}}_k^T}{\rho + 1}, & \text{if } k > 0, \end{cases} \quad (26)$$

where ρ represents a forgetting factor and usually set as $\rho = 0.98$ [32].

The matrix \mathbf{L}_k in (23) is designed as follows

$$\mathbf{L}_k = \lambda (\boldsymbol{\eta}_k - \varphi_{\max}^{-2} \mathbf{I})^{\frac{1}{2}}, \quad (27)$$

where $(\cdot)^{\frac{1}{2}}$ denotes the matrix square root, $\varphi_{\max}^2 \mathbf{I}$ indicates the upper bound of the $\hat{\mathbf{P}}_k$, which can be obtained from the information of practical systems.

Remark 2: It should be noted that the bound of $\hat{\mathbf{x}}_k$ can be controlled by enlarging the estimation error covariance matrix $\hat{\mathbf{P}}_k$. Therefore, an appropriate design of the matrix \mathbf{L}_k is vital to the robust ability of the proposed method. In [19] and [33], by designing \mathbf{L}_k as an identity matrix \mathbf{I} , $\hat{\mathbf{P}}_k$ could be enlarged by decreasing λ , but it is difficult to choose a suitable λ to guarantee $\hat{\mathbf{P}}_k$ is sufficiently large. In order to deal with this problem, a novel method is proposed to design matrix \mathbf{L}_k in (27), by which not only the difficulty of tuning the parameter λ is avoided, but also the requirements of $\hat{\mathbf{P}}_k$ can be satisfied.

Remark 3: It is worth pointing out that the use of the upper bound $\varphi_{\max}^2 \mathbf{I}$ might be too conservative, due to the overemphasis of accommodating the worst condition (largest uncertainties) at the cost of optimality of the method. Thus, in order to improve the robustness of the proposed method without decreasing accuracy, a novel adaptive strategy that makes $\hat{\mathbf{P}}_k$ adapt to the dynamically changing environment is proposed in (23). With this specific design, while the innovation is large, the estimation error covariance matrix $\hat{\mathbf{P}}_k$ will be set as $(\boldsymbol{\eta}_k - \lambda^{-2} \mathbf{L}_k^T \mathbf{L}_k)^{-1}$ to avoid the proposed method divergence; on the other hand, while the innovation is small, $\hat{\mathbf{P}}_k$ will be set as $(\mathbf{I} - \mathbf{K}_k \mathbf{H}_k) \tilde{\mathbf{P}}_k$, so that the estimation will not be distorted.

C. Estimation of Covariance Matrices $\boldsymbol{\xi}_k$ and \mathbf{R}_k

For a practical power system, the noise covariance matrices $\boldsymbol{\xi}_k$ and \mathbf{R}_k are heavily depending on the actual operating conditions of the system and changing from time to time. Therefore, in order to further enhance the robustness of the proposed method and accommodate the changeable noise environment of power system, the covariance matrices of process noise and measurement noise should be estimated dynamically at each time instant.

In order to dynamically calculate the covariance matrices of process noise and measurement noise, it follows from [34], [35] that a modified Sage-Husa noise estimator is developed, which can be summarized as the following steps:

Step 1: Calculate the innovation sequence $\tilde{\mathbf{z}}_k$ by

$$\tilde{\mathbf{z}}_k = \mathbf{z}_k - \mathbf{h}(\tilde{\mathbf{x}}_k), \quad (28)$$

Algorithm 1: Adaptive H_∞ Extended Kalman Filter.

- 1: Parameter Identification: identify the parameters of matrices \mathbf{F}_{k-1} and \mathbf{G}_{k-1} ;
- 2: Initialization: set initial values for $\hat{\mathbf{x}}_0, \hat{\mathbf{P}}_0, \hat{\boldsymbol{\xi}}_0, \hat{\mathbf{R}}_0, S_t$;
- 3: Input: measurement \mathbf{z}_k ;
- 4: **for** $k = 0$ to S_t **do**
- 5: calculate the prediction state vector
- 6: $\hat{\mathbf{x}}_k \leftarrow \mathbf{F}_{k-1}\hat{\mathbf{x}}_{k-1} + \mathbf{G}_{k-1}$;
- 7: compute the prediction error covariance matrix
- 8: $\tilde{\mathbf{P}}_k \leftarrow \mathbf{F}_{k-1}\hat{\mathbf{P}}_{k-1}\mathbf{F}_{k-1}^T + \hat{\boldsymbol{\xi}}_{k-1}$;
- 9: calculate the gain of Kalman filter
- 10: $\mathbf{K}_k \leftarrow \tilde{\mathbf{P}}_k\mathbf{H}_k^T(\mathbf{H}_k\tilde{\mathbf{P}}_k\mathbf{H}_k^T + \hat{\mathbf{R}}_k)^{-1}$;
- 11: update the predicted state vector with measurement \mathbf{z}_k
- 12: $\hat{\mathbf{x}}_k \leftarrow \hat{\mathbf{x}}_k + \mathbf{K}_k[\mathbf{z}_k - \mathbf{h}(\hat{\mathbf{x}}_k)]$;
- 13: compute the matrices $\boldsymbol{\eta}_k, \mathbf{P}_{z,k}$ and $\tilde{\mathbf{P}}_{z,k}$;
- 14: adaptive update the estimation error covariance matrix
- 15: $\hat{\mathbf{P}}_k \leftarrow \begin{cases} (\mathbf{I} - \mathbf{K}_k\mathbf{H}_k)\tilde{\mathbf{P}}_k & \text{if } \mathbf{P}_{z,k} > \alpha\tilde{\mathbf{P}}_{z,k}, \\ (\boldsymbol{\eta}_k - \lambda^{-2}\mathbf{L}_k^T\mathbf{L}_k)^{-1} & \text{otherwise,} \end{cases}$
- 16: estimate the covariance matrix of system noise
- 17: $\hat{\boldsymbol{\xi}}_k \leftarrow (1 - d_{k-1})\hat{\boldsymbol{\xi}}_{k-1} + d_{k-1}(\mathbf{K}_k\tilde{\mathbf{z}}_k\tilde{\mathbf{z}}_k^T\mathbf{K}_k^T + \hat{\mathbf{P}}_k)$;
- 18: estimate the covariance matrix of measurement noise
- 19: $\hat{\mathbf{R}}_{k+1} \leftarrow \hat{\mathbf{R}}_k \cdot \exp^{|\tilde{\mathbf{z}}_{k+1}|}$;
- 20: **end for**

where $\tilde{\mathbf{z}}_k$ and \mathbf{z}_k represent the innovation and real measurement, respectively. $\mathbf{h}(\hat{\mathbf{x}}_k)$ indicates the predicted measurement at time instant k .

Step 2: Estimate the covariance matrix of process noise $\boldsymbol{\xi}_k$ by

$$d_{k-1} = \frac{1 - \mathbf{b}}{1 - \mathbf{b}^{k+1}} \quad (29)$$

$$\hat{\boldsymbol{\xi}}_k = (1 - d_{k-1})\hat{\boldsymbol{\xi}}_{k-1} + d_{k-1}(\mathbf{K}_k\tilde{\mathbf{z}}_k\tilde{\mathbf{z}}_k^T\mathbf{K}_k^T + \hat{\mathbf{P}}_k), \quad (30)$$

where \mathbf{b} is a constant parameter, which usually can be chosen from the interval $[0.95, 0.995]$ under slowly changing characteristics of system noise; $\hat{\boldsymbol{\xi}}_k$ represents the estimation covariance matrix of process noise, $\hat{\mathbf{P}}_k$ indicates the state estimation error covariance matrix at time instant k .

Step 3: Compute the covariance matrix of measurement noise $\hat{\mathbf{R}}_k$ according to the following formula

$$\hat{\mathbf{R}}_k(i, i) = \hat{\mathbf{R}}_{k-1}(i, i) \cdot \exp^{|\tilde{\mathbf{z}}_k(i)|}, \quad (31)$$

where $\hat{\mathbf{R}}_k(i, i)$ represents the i th diagonal element of the estimation covariance of measurement noise, $\tilde{\mathbf{z}}_k(i)$ indicates the i th innovation at time instant k , \exp denotes the exponential function with the natural constant e as the base.

For convenience, the proposed forecasting-aided state estimation for power system against uncertainties is fully summarized as Algorithm 1.

TABLE I
MEASUREMENT CONFIGURATION FOR THE TEST SYSTEMS

Test system	NS	NPJ	NPF	NV	Redundancy
IEEE 14-bus	27	10	34	5	1.81
IEEE 30-bus	59	17	78	15	1.86
IEEE 57-bus	113	38	148	10	1.73
IEEE 118-bus	235	40	352	10	1.71

Remark 4: Based on the innovation information sequence, a modified Sage-Husa noise estimator is designed. By using this method, the covariance matrices of process noise and measurement noise can be adjusted dynamically with the actual operating conditions of the power system, which further enhances the robustness and stability of the proposed method, and a much better estimation performance can be achieved.

IV. NUMERICAL RESULTS

In this section, extensive numerical simulations are carried out on different IEEE benchmark test systems with wind farms integration for verifying the performance of the proposed method.

A. Test Systems

In order to validate the robustness and effectiveness of the proposed method, extensive simulations are carried out on the IEEE 14, 30, 57 and 118-bus systems. The scaled 24-min load coefficient, the generation participation factor and wind data in [36] are utilized for simulations. The 24-min interval is filled with 144 samples, which is similar to the simulations carried out in [2]. Note that the generator outputs are changed according to the assignment of the participation factors. Then, the dynamic variation of power systems can be simulated by successfully running load flows at each time sample with different loading conditions. The outcome of the power flows serve as true values of measurements (\mathbf{z}_k) and true states (\mathbf{x}_k) that includes line flows, bus injections and bus voltages. Then, the actual measurements can be obtained by adding \mathbf{z}_k with random Gaussian noises.

The measurement configuration for the different test systems are provided in Table I, where NS, NPJ, NPF, and NV denote the number of states, power injections, power flow and voltage measurements, respectively. The selection of the two smoothing parameters is important for the accuracy of state prediction model (3). In our research, they are estimated by the method in [38] and the identified results of them are $\alpha = 0.601$ and $\beta = 10^{-5}$, respectively. The threshold for the convergence is 10^{-4} . All the tests are implemented in MATLAB environment using a computer with Intel Core CPU i5-6500 @ 3.2 GHz and 8-GB RAM.

In these test systems, the following four comparative experiments are carried out:

Case Study 1: The proposed AHEKF approach, HEKF [19] and EKF [25] are implemented for the test systems with fully known and accurate parameters.

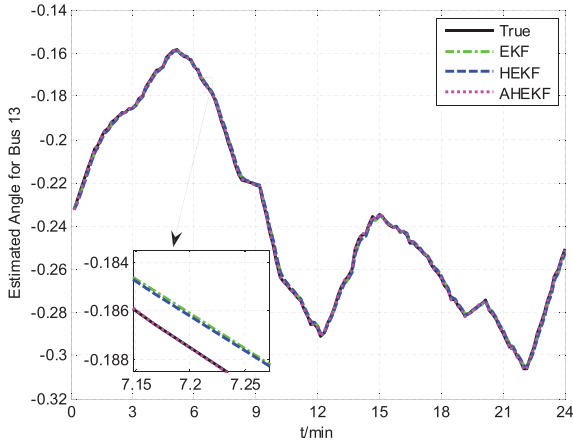


Fig. 1. Estimated results of the voltage angle at Bus 13 in IEEE 118-bus test system by using different methods for Case Study 1.

Case Study 2: When the two smoothing parameters are unknown, the uncertainties of them are considered as 15%–20%, the discussed approaches are conducted on the all test systems.

Case Study 3: The noise statistics of process noise and measurement noise are unknown. The initial variances of process noise and measurement noise are set as 10^{-2} , 10^{-3} respectively, while their corresponding true values are 10^{-4} , 10^{-5} .

Case Study 4: The efficacy of the discussed approaches against sudden load change are compared.

In addition, in order to obtain more general and significant simulation results, $N_{MC} = 100$ Monte-Carlo simulations are run in all case studies. The notion of mean relative error (MRE) is adopted to evaluate the performance of the proposed method and the approaches in [19], [25]. The MRE of estimated voltage angle $\hat{\theta}_{MRE}$ and voltage magnitude \hat{V}_{MRE} can be expressed by

$$\hat{\theta}_{MRE} = \frac{1}{N_{MC}} \sum_{j=1}^{N_{MC}} \frac{1}{N_{\theta}} \sum_{i=1}^{N_{\theta}} \frac{|\hat{\theta}_i - \theta_i|}{|\theta_i|}, \quad (32)$$

$$\hat{V}_{MRE} = \frac{1}{N_{MC}} \sum_{j=1}^{N_{MC}} \frac{1}{N_V} \sum_{i=1}^{N_V} \frac{|\hat{V}_i - V_i|}{|V_i|}, \quad (33)$$

where θ_i , $\hat{\theta}_i$ represent the true and estimated voltage angle of the i th bus, respectively; V_i , \hat{V}_i indicate the true and estimated voltage magnitude value of the i th bus, respectively; N_{θ} denotes the number of voltage angles, N_V represents the total number of voltage magnitudes.

B. Case Study 1: Normal Operating Condition

In this case study, the test systems at normal operating condition are taken into account, where the parameters of the test systems are assumed to be known exactly. The estimated results of the voltage angle and voltage magnitude at Bus 13 in IEEE 118-bus test system by using HEKF [19], EKF [25] and the proposed approach are shown in Figs. 1 and 2, respectively. It can be observed that the proposed approach can track the trajectory of voltage changes accurately, and provides the superior performance compared with the other two methods. Due to the fact

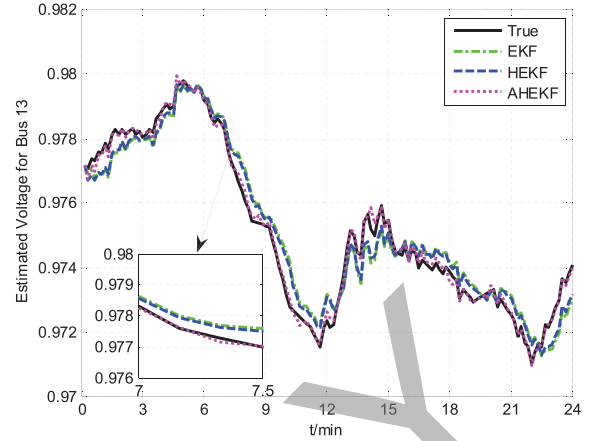


Fig. 2. Estimated results of the voltage magnitude at Bus 13 in IEEE 118-bus test system by using different methods for Case Study 1.

TABLE II
COMPARISON OF ESTIMATION ERROR FOR VOLTAGE ANGLES IN DIFFERENT TEST SYSTEMS

Method	14-bus	30-bus	57-bus	118-bus
EKF	0.0119	0.0251	0.0276	0.0281
HEKF	0.0117	0.0238	0.0247	0.0253
AHEKF	0.0006	0.0027	0.0028	0.0032

TABLE III
COMPARISON OF ESTIMATION ERROR FOR VOLTAGE MAGNITUDES IN DIFFERENT TEST SYSTEMS

Method	14-bus	30-bus	57-bus	118-bus
EKF	0.0016	0.0041	0.0045	0.0048
HEKF	0.0014	0.0037	0.0039	0.0041
AHEKF	0.0007	0.0009	0.0012	0.0015

that it can adaptively update both the state estimation error covariance matrix and noise covariance matrices simultaneously, which can mitigate and suppress the state estimation error caused by the linearization. In addition, the HEKF method presents a little better performance than EKF, which only considers the uncertainties.

In addition, in order to further demonstrate the efficacy of the proposed method, extensive simulations are also conducted on the other test systems. The state estimation results of all the test systems are shown in Tables II–III, which show that the proposed method is able to obtain the most accurate estimation results compared with HEKF and EKF. These results further prove the superior performance of the proposed method.

C. Case Study 2: Uncertain Parameters of State-Space Model

In this subsection, in order to investigate the effects of uncertainties on the performance of each discussed approach, the values of two smoothing parameters α , β are assumed not identified exactly. The uncertainty of their values are considered to be 15%~20% (the true value of them are 0.601 and 10^{-5} , respectively).

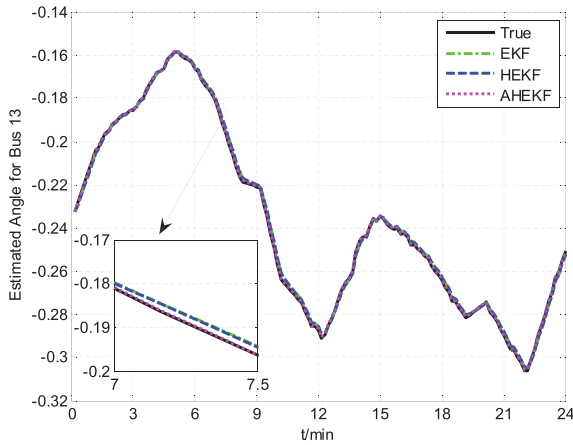


Fig. 3. Estimated results of the voltage angle at Bus 13 in IEEE 118-bus test system for Case Study 2.

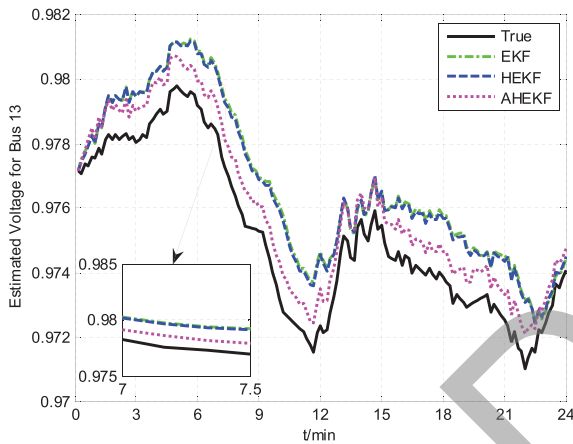


Fig. 4. Estimated results of the voltage magnitude at Bus 13 in IEEE 118-bus test system for Case Study 2.

TABLE IV
COMPARISON OF ESTIMATION ERROR FOR VOLTAGE ANGLES IN
DIFFERENT TEST SYSTEMS

Method	14-bus	30-bus	57-bus	118-bus
EKF	0.0121	0.0264	0.0281	0.0287
HEKF	0.0118	0.0245	0.0253	0.0256
AHEKF	0.0009	0.0030	0.0031	0.0039

Figs. 3 and 4 display the estimated results of voltage angle and voltage magnitude at Bus 13 in IEEE 118-bus test system, respectively. In addition, the other test results are also provided in Tables IV and V. From these test results, it can be found that the estimation errors of EKF, HEKF and the proposed method increase obviously if compared with the normal operation scenario. Specifically, the estimated results provided by the EKF method are biased significantly as it is not taken into account the effects of parameter uncertainties. Both the proposed method and HEKF method outperform the EKF approach, due to their robustness, they are able to effectively mitigate the bad effects by parameters uncertainties. In addition, as expected,

TABLE V
COMPARISON OF ESTIMATION ERROR FOR VOLTAGE MAGNITUDES IN
DIFFERENT TEST SYSTEMS

Method	14-bus	30-bus	57-bus	118-bus
EKF	0.0033	0.0058	0.0061	0.0067
HEKF	0.0027	0.0057	0.0059	0.0064
AHEKF	0.0014	0.0018	0.0023	0.0027

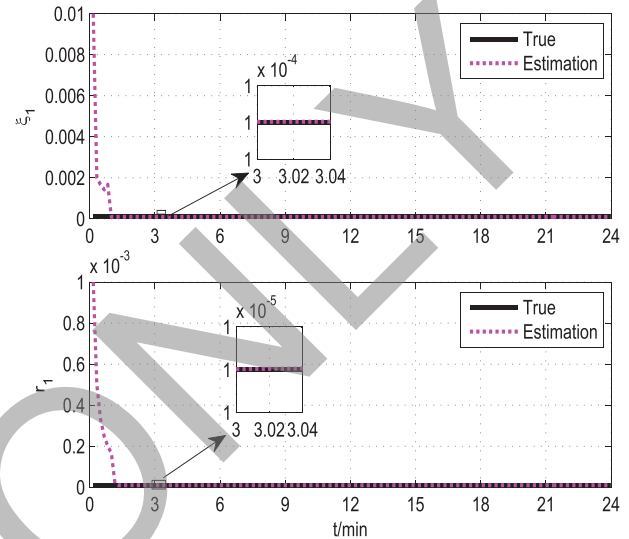


Fig. 5. Estimated results of the component of system noise covariance matrix ξ_1 and the component of measurement noise covariance matrix r_1 in IEEE 118-bus test system for Case Study 3.

the proposed method presents much better performance than HEKF, since its estimation covariance matrix shown in (23) can be dynamically adjusted to the best status according to the changing environment, which could mitigate the adverse effect of the uncertain model parameters more effectively. Therefore, it is not surprising that the AHEKF approach outperforms the HEKF method and shows more robust to the uncertainties of model parameters.

D. Case Study 3: Uncertain Noise Statistics

In this scenario, the noise statistics of the process and measurement noise are assumed unknown. The covariance matrices of process noise and measurement noise are set as $10^{-2}\mathbf{I}$ and $10^{-3}\mathbf{I}$ with appropriate dimensions, respectively, while the corresponding true values of them are $10^{-4}\mathbf{I}$ and $10^{-5}\mathbf{I}$.

In order to show the efficiency of the noise statistic estimator, the estimated results of the components of process and measurement noise covariance matrices are shown in Figs. 5 and 6 (actually, all the estimated results of the noise covariance matrices have been analyzed and the simulation results are similar. Therefore, due to the page limit, only two elements of the covariance matrices are randomly selected and presented). As can be seen from the results shown in Figs. 5 and 6, the developed method could revise the noise covariance matrices accurately and timely, which is important for effectively bounding their

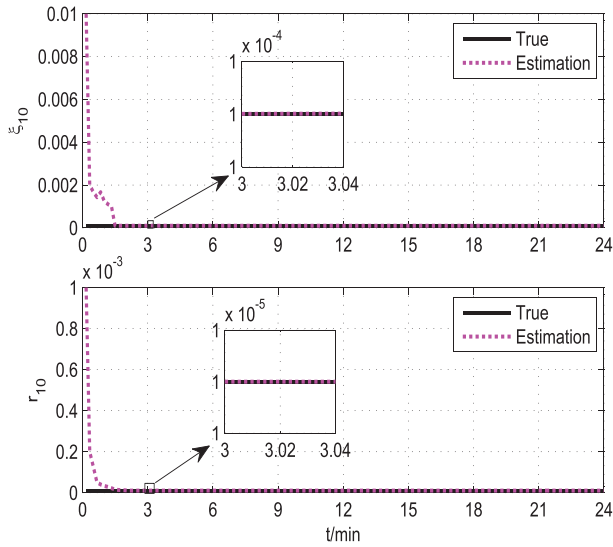


Fig. 6. Estimated results of the component of system noise covariance matrix ξ_{10} and the component of measurement noise covariance matrix r_{10} in IEEE 118-bus test system for Case Study 3.

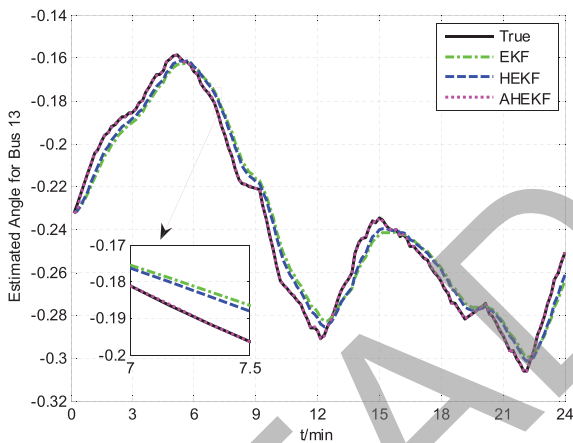


Fig. 7. Estimated results of the voltage angle at Bus 13 in IEEE 118-bus test system for Case Study 3.

adverse effects. Then, the estimated results of voltage angle and magnitude at Bus 13 in IEEE 118-bus are shown in Figs. 7 and 8, respectively. The estimated error results of all the test systems are also presented in Tables VI and VII. It can be observed from these test results that the performance of the three approaches are heavily affected by the mismatched initial covariance matrices of process noise and measurement noise if compared with the normal operation condition. Specifically, the performance of EKF method are degraded the most severely. HEKF method outperforms EKF, due to it can bound the estimation errors to some extent. However, HEKF method can not correct the mismatched initial covariance matrixes dynamically and adaptively update the estimation covariance matrix with responding to the changeable conditions, thus the estimation errors are still large. With the utilization of the dynamic correction technique, the proposed method achieves the best performance of the three methods, which exhibits strong robustness to the

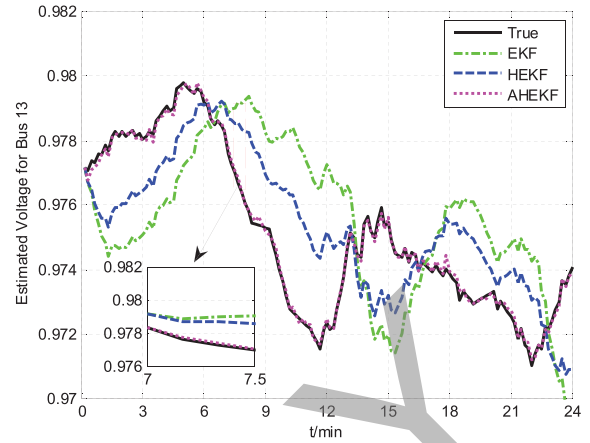


Fig. 8. Estimated results of the voltage magnitude at Bus 13 in IEEE 118-bus test system for Case Study 3.

TABLE VI
COMPARISON OF ESTIMATION ERROR FOR VOLTAGE ANGLES IN
DIFFERENT TEST SYSTEMS

Method	14-bus	30-bus	57-bus	118-bus
EKF	0.0129	0.0311	0.0319	0.0324
HEKF	0.0127	0.0304	0.0309	0.0317
AHEKF	0.0003	0.0027	0.0028	0.0039

TABLE VII
COMPARISON OF ESTIMATION ERROR FOR VOLTAGE MAGNITUDES IN
DIFFERENT TEST SYSTEMS

Method	14-bus	30-bus	57-bus	118-bus
EKF	0.0048	0.0117	0.0127	0.0139
HEKF	0.0039	0.0102	0.0116	0.0128
AHEKF	0.0008	0.0009	0.0012	0.0017

noise uncertainties. These comparisons further prove the superior performance of the proposed method.

E. Case Study 4: Sudden Load Change

In this case, in order to further demonstrate the robustness of the proposed method, the sudden load change of system is also investigated. It is assumed that the active power of the load at Bus 5 in IEEE 14 test system changes from 0.076 p.u. to 0.4 p.u. during $t = 1.67$ min and $t = 2$ min (actually, the three approaches have been tested in the all test systems with sudden load change, and the simulation results are consistent with the test results in IEEE 14-bus test system. However, due to the page limit, only the results of IEEE 14-bus are presented).

The simulation results of voltage angle and magnitude at Bus 5 in IEEE 14-bus test system are shown in Figs. 9 and 10, respectively. Due to the voltage angle and magnitude are closely related to the change of active and reactive power, therefore, the sudden load change will cause large variations in the voltage angle and magnitude. This can be observed through the test results from the time $t = 1.67$ min to $t = 2$ min, where the

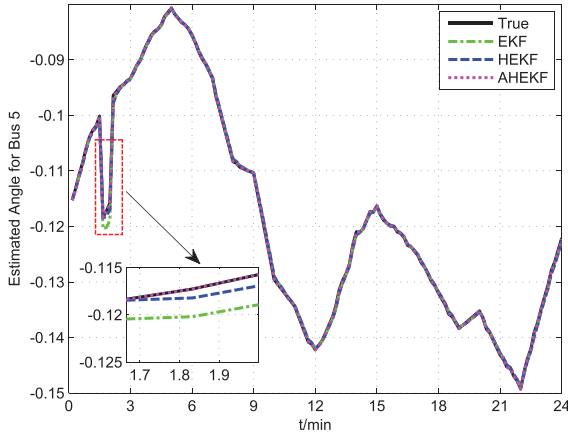


Fig. 9. Estimated results of the voltage angle at Bus 5 in IEEE 14-bus test system for Case Study 4.

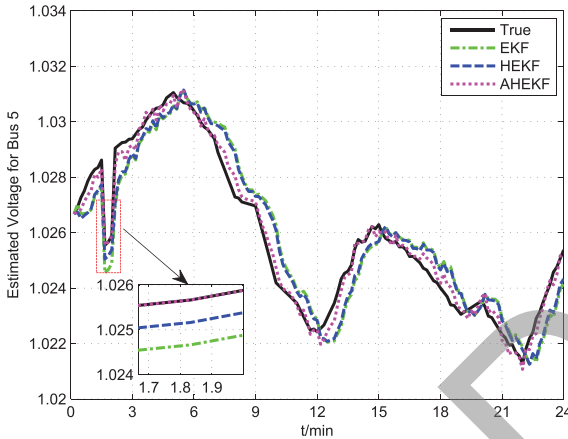


Fig. 10. Estimated results of the voltage magnitude at Bus 5 in IEEE 14-bus test system for Case Study 4.

voltage angle and magnitude at Bus 5 are with large variations when the load change occurs. It is obviously seen that, with sudden load change, both EKF and HEKF can not track the dynamic changes of the voltage angle and magnitude accurately. However, the proposed method can effectively track the dynamics by adaptively updating the estimation covariance matrix and noise covariance matrices, which exhibits strong robustness.

V. CONCLUSION

Accurate forecasting-aided state estimation is paramount for power system monitoring and control, especially with volatile renewable generation. In this paper, a novel robust adaptive H_∞ extended Kalman filter for power system forecasting-aided state estimation against uncertainties was proposed. It mainly has the following advantages: (i) the modified innovation based Sage-Husa estimator of noise statistics can dynamically revise the covariance matrices of process noise and measurement noise timely and accurately, which plays an important role in bounding the adverse effects of noise statistical uncertainties; (ii) based on the H_∞ criteria in robust control theory and the adaptive technique, an adaptive strategy was designed to automatically

tune the estimation error covariance matrix with respecting to the changeable conditions. As a result, not only the difficulty of choosing a suitable upper bound of state estimation error is avoided and but also a higher accuracy of forecasting-aided state estimation can be achieved. Extensive simulation tests carried out on the different IEEE benchmark test systems under various situations demonstrated the effectiveness and robustness of the proposed method.

APPENDIX

In this section, more detailed derivations of the state estimation covariance matrix in (23) and the stability analysis of the proposed AHEKF method are presented.

A. Derivation of the Estimation Covariance Matrix

It is worth pointing out that the solution of the objective function in (15) could be presented to be equivalent to that of Krein space Kalman filter [39]. By converting the suboptimal H_∞ filtering problem to an indefinite form, then the Krein space Kalman filter can be utilized [40]. Formally, we get

$$\begin{aligned}
 J_\infty &= \|\mathbf{x}_0 - \hat{\mathbf{x}}_0\|_{\hat{\mathbf{P}}_0^{-1}}^2 + \sum_{k=0}^{N_t-1} \|\mathbf{w}_k\|_{\hat{\boldsymbol{\xi}}_k^{-1}}^2 + \sum_{k=0}^{N_t-1} \|\mathbf{v}_k\|_{\hat{\mathbf{R}}_k^{-1}}^2 \\
 &\quad - \lambda^2 \sum_{k=0}^{N_t-1} \|\mathbf{x}_k - \hat{\mathbf{x}}_k\|_{\hat{\mathbf{P}}_k^{-1}}^2 \\
 &= \|\mathbf{x}_0 - \hat{\mathbf{x}}_0\|_{\hat{\mathbf{P}}_0^{-1}}^2 + \sum_{k=0}^{N_t-2} \|\mathbf{w}_k\|_{\hat{\boldsymbol{\xi}}_k^{-1}}^2 \\
 &\quad + \sum_{k=0}^{N_t-1} \begin{bmatrix} \mathbf{z}_k - \mathbf{h}(\mathbf{x}_k) \\ \mathbf{x}_k - \hat{\mathbf{x}}_k \end{bmatrix}^T \begin{bmatrix} \hat{\mathbf{R}}_k & 0 \\ 0 & -\lambda^2 \mathbf{L}_k^T \mathbf{L}_k \end{bmatrix}^{-1} \\
 &\quad \begin{bmatrix} \mathbf{z}_k - \mathbf{h}(\mathbf{x}_k) \\ \mathbf{x}_k - \hat{\mathbf{x}}_k \end{bmatrix}, \tag{34}
 \end{aligned}$$

On the other hand, the system function (1) and measurement function (2) are linearized using a first-order Taylor series expansion at the predicted state vector $\tilde{\mathbf{x}}_k$, yielding

$$\mathbf{x}_k = \bar{\mathbf{F}}_k \mathbf{x}_{k-1} + \tilde{\mathbf{x}}_k - \bar{\mathbf{F}}_k \tilde{\mathbf{x}}_{k-1} + \mathbf{w}_k, \tag{35}$$

$$\mathbf{z}_k = \mathbf{H}_k \mathbf{x}_k + \tilde{\mathbf{z}}_k - \mathbf{H}_k \tilde{\mathbf{x}}_k + \mathbf{v}_k, \tag{36}$$

where $\bar{\mathbf{F}}_k$, \mathbf{H}_k indicate the Jacobian matrices of system and measurement function, respectively; $\tilde{\mathbf{z}}_k = \mathbf{h}(\tilde{\mathbf{x}}_k)$ represents the predicted measurement at time instant k .

Then, by substituting formulas (35) and (36) into (34) and following the steps of the Krein space Kalman filter [39], the state estimation error covariance matrix that satisfies the criteria (15) can be derived as follows

$$\hat{\mathbf{P}}_k = (\boldsymbol{\eta}_k - \lambda^{-2} \mathbf{L}_k^T \mathbf{L}_k)^{-1} \tag{37}$$

where $\mathbf{L}_k \in \mathbb{R}^{n \times n}$ represents a matrix to be designed, $\boldsymbol{\eta}_k$ and $\mathbf{P}_{z,k}$ are calculated by

$$\boldsymbol{\eta}_k = \tilde{\mathbf{P}}_k^{-1} + \mathbf{H}_k^T \hat{\mathbf{R}}_k^{-1} \mathbf{H}_k, \tag{38}$$

$$\mathbf{P}_{z,k} = \mathbf{H}_k \tilde{\mathbf{P}}_k \mathbf{H}_k^T + \hat{\mathbf{R}}_k. \tag{39}$$

In [19] and [33], by designing \mathbf{L}_k as an identity matrix \mathbf{I} with an appropriate dimension, $\hat{\mathbf{P}}_k$ could be enlarged by decreasing λ . However, it may be impossible to select a suitable λ such that $\hat{\mathbf{P}}_k$ is sufficiently large. Moreover, the modulation of λ is another difficulty. In fact, these problems can be solved by design the matrix \mathbf{L}_k as

$$\mathbf{L}_k = \lambda(\boldsymbol{\eta}_k - \varphi_{\max}^{-2} \mathbf{I})^{\frac{1}{2}}, \quad (40)$$

where $(\cdot)^{\frac{1}{2}}$ denotes the matrix square root, $\varphi_{\max}^2 \mathbf{I}$ indicates the upper bound of the $\hat{\mathbf{P}}_k$, which can be obtained from the information of practical systems.

Nevertheless, the utilization of the upper bound $\varphi_{\max}^2 \mathbf{I}$ might be too conservative, due to the overemphasis of accommodating the worst condition (largest uncertainties) at the cost of optimality of the method. Thus, in order to improve the robustness of the proposed method without decreasing accuracy, a novel adaptive strategy that makes $\hat{\mathbf{P}}_k$ adapt to the dynamically changing environment is proposed in (23).

B. Stability Analysis of the Proposed AHEKF Method

In the part, based on the final results in [41]–[43], the stability and convergence properties of the proposed AHEKF approach are investigated. At first, by utilizing the Taylor series, the system function \mathbf{f} and measurement function \mathbf{h} can be expanded to the linear and nonlinear parts as

$$\mathbf{f}(\mathbf{x}_k) - \mathbf{f}(\hat{\mathbf{x}}_k) = \bar{\mathbf{F}}_k(\mathbf{x}_k - \hat{\mathbf{x}}_k) + \boldsymbol{\varphi}(\mathbf{x}_k, \hat{\mathbf{x}}_k), \quad (41)$$

$$\mathbf{h}(\mathbf{x}_k) - \mathbf{h}(\hat{\mathbf{x}}_k) = \mathbf{H}_k(\mathbf{x}_k - \hat{\mathbf{x}}_k) + \boldsymbol{\chi}(\mathbf{x}_k, \hat{\mathbf{x}}_k), \quad (42)$$

where $\bar{\mathbf{F}}_k$ and \mathbf{H}_k represent the Jacobian matrices of system and measurement function, respectively. $\boldsymbol{\varphi}$ and $\boldsymbol{\chi}$ denote the nonlinear parts.

For convenience, the estimation error is defined as

$$\boldsymbol{\zeta}_k = \mathbf{x}_k - \hat{\mathbf{x}}_k, \quad (43)$$

where $\boldsymbol{\zeta}_k$ represents the estimation error.

Based on the research results in [39] and [41], the sufficient conditions to ensure the stability of the AHEKF approach are demonstrated in the following theorem.

Theorem 1: Consider the discrete time state-space model shown in (1) and (2), and the proposed approach as stated in (16)–(23). Let the following assumptions hold for all $k > 0$

- (a) There are positive real numbers $\bar{f}, \bar{h}, \bar{p}, \bar{q}, \bar{r} > 0$, such that the following bounds are fulfilled

$$\begin{aligned} \|\bar{\mathbf{F}}_k\| &\leq \bar{f}, \quad \|\mathbf{H}_k\| \leq \bar{h}, \\ \bar{p}\mathbf{I} &\leq \hat{\mathbf{P}}_k \leq \bar{p}\mathbf{I}, \quad \bar{q}\mathbf{I} \leq \boldsymbol{\xi}_k, \quad \bar{r}\mathbf{I} \leq \mathbf{R}_k. \end{aligned} \quad (44)$$

- (b) $\bar{\mathbf{F}}_k$ is a nonsingular matrix.
(c) There are positive real numbers $\epsilon_\varphi, \epsilon_\chi, \kappa_\varphi, \kappa_\chi > 0$ such that the nonlinear functions $\boldsymbol{\varphi}$ and $\boldsymbol{\chi}$ is able to be bounded as

$$\|\boldsymbol{\varphi}(\mathbf{x}_k, \hat{\mathbf{x}}_k)\| \leq \kappa_\varphi \|\mathbf{x}_k - \hat{\mathbf{x}}_k\|^2, \quad (45)$$

$$\|\boldsymbol{\chi}(\mathbf{x}_k, \hat{\mathbf{x}}_k)\| \leq \kappa_\chi \|\mathbf{x}_k - \hat{\mathbf{x}}_k\|^2, \quad (46)$$

for $\mathbf{x}_k, \hat{\mathbf{x}}_k \in \mathbf{R}^p$ with $\|\mathbf{x}_k - \hat{\mathbf{x}}_k\| \leq \epsilon_\varphi$ and $\|\mathbf{x}_k - \hat{\mathbf{x}}_k\| \leq \epsilon_\chi$.

Then the forecasting-aided state estimation error $\boldsymbol{\zeta}_k$ is exponentially bounded in mean square and bounded with probability one, provided that the initial state estimation error satisfies

$$\|\boldsymbol{\zeta}_k\| \leq \epsilon, \quad (47)$$

for some $\epsilon > 0$.

In practical power system, the conditions of noise covariance matrices and state estimation error covariance matrices in (44) are obvious satisfied and can be easily verified in practice. Therefore, in what follows, the remaining conditions in Theorem 1 are analyzed to investigate the stability property of the proposed method.

Proof:

(1) Constraints on the Linearized System Matrix

According to Theorem 1, the linearized matrix $\bar{\mathbf{F}}_k$ needs to satisfy the conditions that: (i) the norm of it should have an upper bound; (ii) it is a nonsingular matrix. The infinite norm of $\bar{\mathbf{F}}_k$ is

$$\|\bar{\mathbf{F}}_k\|_\infty = \max_i \sum_{j=1}^n |\bar{F}_{k,i,j}|. \quad (48)$$

If each element of $\bar{\mathbf{F}}_k$ is bounded for all k , then its infinite norm can be bounded for all k . It can easily derived from (6) that all the elements of $\bar{\mathbf{F}}_k$ are constants, therefore, $\bar{\mathbf{F}}_k$ is clearly upper bound. And the same constraints on \mathbf{H}_k can also be verified from the measurement equations in (11)–(14).

In addition, due to $\bar{\mathbf{F}}_k$ have full rank for all $k > 0$, therefore, the nonsingular constraint on it is satisfied.

(2) Lipschitz Bounded Nonlinear Functions

The last condition for the forecasting-aided state estimation error $\boldsymbol{\zeta}_k$ to be exponentially bounded is that the inequalities presented in (45), (46) must be satisfied. In the forecasting-aided state estimation model utilized, the system function $\mathbf{f}(\mathbf{x}_k)$ is linear, so $\boldsymbol{\varphi} = 0$ and thus the inequality clearly holds for this function. In addition, to investigate the inequality for the function $\boldsymbol{\chi}$, the j th element of $\boldsymbol{\chi}$ can be expanded as follows

$$\chi_j(\mathbf{x}_k, \hat{\mathbf{x}}_k) = \frac{1}{2}(\mathbf{x}_k - \hat{\mathbf{x}}_k)^T \left(\frac{\partial^2 \mathbf{h}_j}{\partial \mathbf{x}_k^2}(\hat{\mathbf{x}}_k) + \dots \right) (\mathbf{x}_k - \hat{\mathbf{x}}_k). \quad (49)$$

Utilizing the triangular inequality

$$\|\chi_j(\mathbf{x}_k, \hat{\mathbf{x}}_k)\| \leq \left\| \frac{1}{2} \left(\frac{\partial^2 \mathbf{h}_j}{\partial \mathbf{x}_k^2}(\hat{\mathbf{x}}_k) + \dots \right) \right\| \|\mathbf{x}_k - \hat{\mathbf{x}}_k\|^2, \quad (50)$$

since all elements in the derivatives of \mathbf{h} are bounded for all $k > 0$, therefore, there is a constant E_j such that

$$\|\chi_j(\mathbf{x}_k, \hat{\mathbf{x}}_k)\| \leq E_j \|\mathbf{x}_k - \hat{\mathbf{x}}_k\|^2 \quad (51)$$

$$\|\chi_j(\mathbf{x}_k, \hat{\mathbf{x}}_k)\|_\infty = \max_i (E_j) \|\mathbf{x}_k - \hat{\mathbf{x}}_k\|_\infty^2 \quad (52)$$

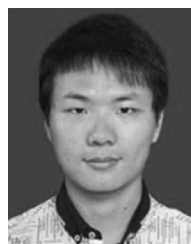
$$\|\chi_j(\mathbf{x}_k, \hat{\mathbf{x}}_k)\| \leq \kappa_\chi \|\mathbf{x}_k - \hat{\mathbf{x}}_k\|^2 \quad (53)$$

where κ_χ represents a positive constant.

It follows from the above analysis that all the conditions in Theorem 1 are fulfilled. Therefore, the forecasting-aided state estimation error ζ_k of the proposed approach is exponentially bounded. ■

REFERENCES

- [1] L. Hu, Z. Wang, I. Rahman, and X. Liu, "A constrained optimization approach to dynamic state estimation for power systems including PMU and missing measurements," *IEEE Trans. Control Syst. Technol.*, vol. 24, no. 2, pp. 703–710, Jan. 2016.
- [2] J. Zhao, G. Zhang, Z. Dong, and M. L. Scala, "Robust forecasting aided power system state estimation considering state correlations," *IEEE Trans. Smart Grid*, vol. 9, no. 4, pp. 2658–2666, Jul. 2018.
- [3] S. Deshmukh, N. Balasubramaniam, and A. Pahwa, "State estimation and voltage/VAR control in distribution network with intermittent measurements," *IEEE Trans. Smart Grid*, vol. 5, no. 1, pp. 200–209, Jan. 2014.
- [4] M. Filho and J. Souza, "Forecasting-aided state estimation—Part I: Panorama," *IEEE Trans. Power Syst.*, vol. 24, no. 4, pp. 1667–1677, Nov. 2009.
- [5] E. Ghahremani and I. Kamwa, "Local and wide-area PMU-based decentralized dynamic state estimation in multi-machine power systems," *IEEE Trans. Power Syst.*, vol. 31, no. 1, pp. 547–562, Nov. 2016.
- [6] J. Zhao, M. Netto, and L. Mili, "A robust iterated extended Kalman filter for power system dynamic state estimation," *IEEE Trans. Power Syst.*, vol. 32, no. 4, pp. 3205–3216, Jul. 2017.
- [7] M. Meng and C. Y. Evrenosoglu, "A regression-based analysis based state transition model for power system dynamic state estimation," in *Proc. North Amer. Power Symp.*, Champaign, IL, USA, Sep. 2012, pp. 1–5.
- [8] Y. Sun *et al.*, "PMU placement for dynamic state tracking of power systems," in *Proc. North Amer. Power Symp.*, Boston, MA, USA, Aug. 2011, pp. 1–7.
- [9] S. Wang, W. Gao, and A. Meliopoulos, "An alternative method for power system dynamic state estimation based on unscented transform," *IEEE Trans. Power Syst.*, vol. 27, no. 2, pp. 942–950, May 2012.
- [10] A. K. Singh and B. C. Pal, "Decentralized dynamic state estimation in power systems using unscented transformation," *IEEE Trans. Power Syst.*, vol. 29, no. 2, pp. 794–804, Aug. 2014.
- [11] G. Anagnostou and B. C. Pal, "Derivative-free Kalman filtering based approaches to dynamic state estimation for power systems with unknown inputs," *IEEE Trans. Power Syst.*, vol. 33, no. 1, pp. 116–130, Jan. 2018.
- [12] G. Valverde and V. Terzija, "Unscented Kalman filter for power system dynamic state estimation," *IET Gener. Transmiss. Distrib.*, vol. 5, no. 1, pp. 29–37, Jan. 2011.
- [13] N. Zhou, D. Meng, and S. Lu, "Estimation of the dynamic states of synchronous machines using an extended particle filter," *IEEE Trans. Power Syst.*, vol. 28, no. 4, pp. 4152–4161, Nov. 2013.
- [14] H. Zhao and T. Tian, "Estimation of the dynamic states of synchronous machines using an extended particle filter," *Power Syst. Technol.*, vol. 38, no. 1, pp. 188–192, Jan. 2014.
- [15] A. Monticelli, *State Estimation in Electric Power Systems: A Generalized Approach*. Berlin, Germany: Springer, 1999.
- [16] M. S. Grewal and A. P. Andrews, *Kalman Filtering*. Hoboken, NJ, USA: Wiley, 2008.
- [17] D. Simon, *Optimal State Estimation*. Hoboken, NJ, USA: Wiley, 2006.
- [18] K. Zhou, J. C. Doyle, and K. Glover, *Robust and Optimal Control*. Englewood Cliffs, NJ, USA: Prentice-Hall, 1996.
- [19] J. Zhao, "Dynamic state estimation with model uncertainties using H_∞ extended Kalman filter," *IEEE Trans. Power Syst.*, vol. 33, no. 1, pp. 1099–1100, Jan. 2018.
- [20] J. Zhao and L. Mili, "Robust unscented Kalman filter for power system dynamic state estimation with unknown noise statistics," *IEEE Trans. Smart Grid*, vol. 10, no. 2, pp. 1215–1224, Mar. 2019.
- [21] Y. Wang, Y. Sun, Z. Wei, and G. Sun, "Parameters estimation of electromechanical oscillation with incomplete measurement information," *IEEE Trans. Power Syst.*, vol. 33, no. 5, pp. 5016–5028, Sep. 2018.
- [22] A. Mohamed and K. Schwarz, "Adaptive Kalman filtering for INS/GPS," *J. Geodesy*, vol. 73, no. 4, pp. 193–203, 1999.
- [23] W. Li, S. Sun, Y. Jia, and J. Du, "Robust unscented Kalman filter with adaption of process and measurement noise covariances," *Digit. Signal Process.*, vol. 48, pp. 93–103, Jan. 2016.
- [24] S. Sarkka and A. Nummenmaa, "Recursive noise adaptive Kalman filtering by variational Bayesian approximations," *IEEE Trans. Autom. Control*, vol. 54, no. 3, pp. 596–600, Mar. 2009.
- [25] A. M. L. de Silva, M. B. D. C. Filho, and J. F. de Queiroz, "State forecasting in electric power systems," *IEE Proc. C Gener. Transmiss. Distrib.*, vol. 130, no. 5, pp. 237–244, Sep. 1983.
- [26] G. Durgaprasad and S. Thakur, "Robust dynamic state estimation of power systems based on M-estimation and realistic modeling of system dynamics," *IEEE Trans. Power Syst.*, vol. 13, no. 4, pp. 1331–1336, Nov. 1998.
- [27] H. Karimipour and V. Dinavahi, "Extended Kalman filter-based parallel dynamic state estimation," *IEEE Trans. Smart Grid*, vol. 6, no. 3, pp. 1539–1549, May 2015.
- [28] A. Sharma, S. C. Srivastava, and S. Chakrabarti, "A cubature Kalman filter based power system dynamic state estimator," *IEEE Trans. Instrum. Meas.*, vol. 66, no. 8, pp. 2036–2045, Aug. 2017.
- [29] Z. Guo, S. Li, X. Wang, and W. Heng, "Distributed point-based Gaussian approximation filtering for forecasting-aided state estimation in power systems," *IEEE Trans. Power Syst.*, vol. 31, no. 4, pp. 2597–2608, Jul. 2016.
- [30] J. D. Glover and M. Sarma, *Power System Analysis and Design*. Boston, MA, USA: PWS-Kent, 1994.
- [31] K. Xiong, H. Zhang, and L. Liu, "Adaptive robust extended Kalman filter for nonlinear stochastic systems," *IET Control Theory Appl.*, vol. 2, pp. 239–250, Mar. 2008.
- [32] M. Bai, D. Zhou, and H. Schwarz, "Identification of generalized friction for an experimental planar two-link flexible manipulator using strong tracking filter," *IEEE Trans. Robot. Autom.*, vol. 15, no. 2, pp. 362–369, Apr. 1999.
- [33] G. A. Einicke and L. B. White, "Robust extended Kalman filtering," *IEEE Trans. Signal Process.*, vol. 47, no. 9, pp. 2596–2599, Sep. 1999.
- [34] K. Myers and B. Tapley, "Adaptive sequential estimation with unknown noise statistics," *IEEE Trans. Autom. Control*, vol. 21, no. 4, pp. 520–523, Aug. 1976.
- [35] R. Mehra, "On the identification of variances and adaptive Kalman filtering," *IEEE Trans. Autom. Control*, vol. 15, no. 2, pp. 175–184, Apr. 1970.
- [36] "Wind generation and total load in the BPA balancing authority," Bonneville Power Admin., Portland, OR, USA, 2012. [Online]. Available: <http://transmission.bpa.gov/business/operations/wind>
- [37] I. L. Rivera, V. Vittal, G. T. Heydt, C. R. Esquivel, and C. Camacho, "A dynamic state estimator based control for power system damping," *IEEE Trans. Power Syst.*, vol. 33, no. 6, pp. 6839–6848, Nov. 2018.
- [38] B. A. Moreno, C. R. Esquivel, M. Glavic, and T. C. Cutsem, "Electric power network state tracking from multirate measurements," *IEEE Trans. Instrum. Meas.*, vol. 67, no. 1, pp. 33–44, Jan. 2018.
- [39] B. Hassibi, A. H. Sayed, and T. Kailath, "Linear estimation in Krein spaces—Part II: Applications," *IEEE Trans. Autom. Control*, vol. 41, no. 1, pp. 34–49, Jan. 1996.
- [40] J. Zhao and L. Mili, "A decentralized H-infinity unscented Kalman filter for dynamic state estimation against uncertainties," *IEEE Trans. Smart Grid*, to be published. doi: [10.1109/TSG.2018.2870327](https://doi.org/10.1109/TSG.2018.2870327).
- [41] K. Reif and R. Unbehauen, "The extended Kalman filter as an exponential observer for nonlinear systems," *IEEE Trans. Signal Process.*, vol. 47, no. 8, pp. 2324–2328, Aug. 1999.
- [42] K. Reif, S. Gunther, E. Yaz, and R. Unbehauen, "Stochastic stability of the discrete-time extended Kalman filter," *IEEE Trans. Autom. Control*, vol. 44, no. 4, pp. 714–728, Apr. 1999.
- [43] K. K. Tønne, "Stability analysis of EKF-based attitude determination and control," M.S. thesis, Dept. Eng. Cybern., Norwegian Univ. Sci. Technol., Trondheim, Norway, 2007.



Yi Wang (S'19) received the B.S. degree from the Luoyang Institute of Science and Technology, Luoyang, China, in 2014. He is currently working toward the Ph.D. degree in electrical engineering with Hohai University, Nanjing, China, and is also with the University of Alberta, Edmonton, AB, Canada, as a Joint Ph.D. student during 2018–2019.

His research interests include theoretical and algorithmic studies in power system state estimation, parameter identification, power system dynamics, signal processing, and cyber security.



Yonghui Sun (M'16) received the Ph.D. degree from the City University of Hong Kong, Hong Kong, in 2010. He is currently a Professor with the College of Energy and Electrical Engineering, Hohai University, Nanjing, China. He has authored more than 60 papers in refereed international journals. His research interests include stability analysis and control of power systems, optimal planning and operation of integrated energy system, optimization algorithms, and data analysis.

Dr. Sun was the recipient of the First Award of Jiangsu Provincial Progress in Science and Technology in 2010 as the Fourth Project Member, and he is an Active Reviewer for many international journals.



Venkata Dinavahi (S'94–M'00–SM'08) received the B.Eng. degree in electrical engineering from the Visveswaraya National Institute of Technology (VNIT), Nagpur, India, in 1993, the M.Tech. degree in electrical engineering from the Indian Institute of Technology (IIT) Kanpur, Kanpur, India, in 1996, and the Ph.D. degree in electrical and computer engineering from the University of Toronto, Ontario, ON, Canada, in 2000. He is currently a Professor with the Department of Electrical and Computer engineering, University of Alberta, Edmonton, AB, Canada. His

research interests include real-time simulation of power systems and power electronic systems, electromagnetic transients, device-level modeling, large-scale systems, and parallel and distributed computing.

READ ONLY